JOURNAL OF VIROLOGY, Aug. 1997, p. 5990–5996 Vol. 71, No. 8
0022-538X/97/$04.00+0

The Role of the Pseudoknot at the 3′ End of Turnip Yellow Mosaic Virus RNA in Minus-Strand Synthesis by the Viral RNA-Dependent RNA Polymerase

B. A. L. M. DEIMAN, R. M. KORTLEVER, AND C. W. A. PLEIJ*

Leiden Institute of Chemistry, Gorlaeus Laboratories, 2300 RA Leiden, The Netherlands

Received 8 January 1997/Accepted 12 May 1997

The tRNA-like structure at the 3′ end of turnip yellow mosaic virus (TYMV) RNA was studied in order to determine the role of this structure in the initiation of minus-strand synthesis in vitro. Deletions in the 5′-to-3′ direction up to the pseudoknot structure did not result in a decrease of transcription efficiency. However, transcription efficiency was reduced twofold when a fragment of 21 nucleotides, comprising the 3′-terminal hairpin, was used as a template. $tRNA^{Phe}$ from yeast, *Escherichia coli* 5S rRNA, and the 3′-terminal 208 nucleotides of alfalfa mosaic virus RNA 3 could not be transcribed by the RNA-dependent RNA polymerase (RdRp) of TYMV. Various mutations in the sequences of loop regions L1 and L2 or of stem region S1 of the pseudoknot were tested to further investigate the importance of the pseudoknot structure. The results were compared with those obtained in an earlier study on aminoacylation with the same mutants (R. M. W. Mans, M. H. van Steeg, P. W. G. Verlaan, C. W. A. Pleij, and L. Bosch, J. Mol. Biol. 223:221–232; 1992). Mutants which still harbor a stable pseudoknot, as proven by probing its structure, have a transcription efficiency very close to that of the wild-type virus. Disruption of the pseudoknot structure, however, gives rise to a drop in transcription efficiency to about 50%. No indications of base-specific interactions between L1, L2, or S1 of the pseudoknot and the RdRp were found.

The 3′ end of the positive-stranded RNA genome of turnip yellow mosaic virus (TYMV) is folded into a "tRNA-like structure" (20). The aminoacyl acceptor arm consists of 12 bp, of which 8 bp are part of a pseudoknotted structure (Fig. 1). The structural similarities result in tRNA-like properties of the viral RNA such as adenylation by ATP:tRNA nucleotidyltransferase (9), aminoacylation with valine by valyl-tRNA synthetase (18), and interactions with elongation factors (8, 10). More recent studies showed that substitutions in the anticodon loop that resulted in decreased valylation also reduced multiplication of the virus, indicating a correlation between valine acceptance activity and viability (22). However, switching the aminoacylation identity from valine to methionine resulted in an infectious virus, meaning that neither specific aminoacylation with valine nor the interaction with valyl-tRNA synthetase is crucial (5). Furthermore, enhancement of genome stability or gene expression also did not seem to be the major role of the tRNA-like structure of TYMV RNA (21). Therefore, as replication starts at the 3′ end of the RNA, this tRNA-like structure, or part of it, is thought to be involved in the initiation of minus-strand synthesis.

We recently published a new method for the isolation and partial purification of the RNA-dependent RNA polymerase (RdRp) of TYMV (3). The RdRp, purified up to and through the glycerol gradient centrifugation step, was proven to be of viral origin and specific for TYMV RNA. After treatment with micrococcal nuclease, the RdRp was shown to be completely dependent on added template RNA and could therefore be used for studies on minimal template requirements for minus-strand synthesis.

The 3′-terminal 83 nucleotides (nt) of TYMV RNA (83-nt fragment in Fig. 1), which includes the complete tRNA-like structure, was already shown to be efficiently transcribed by the RdRp of TYMV in vitro (3). Previously, it was suggested that the minus-strand promoter is probably 38 nt long or shorter, as a fragment consisting of the 3′-terminal 38 nt, containing the pseudoknot structure, could compete with viral RNA (6). We have investigated whether RNA fragments containing fewer than 38 nt from the 3′ terminus of TYMV RNA can be used as templates by the RdRp. Subsequently, we have studied, by mutational analysis, the role of the 3′ pseudoknot structure in the initiation of minus-strand synthesis in vitro. We also discuss the results of in vitro transcription by the RdRp in relation to those of aminoacylation and probing of the structures of the same mutants, as previously presented (12), in order to gain further insight into the role of the pseudoknot in the multiplication of the virus.

MATERIALS AND METHODS

RdRp preparation and RdRp assay. The RdRp was isolated, purified up to and through the glycerol gradient centrifugation step, and treated with micrococcal nuclease as described previously (3). Twenty microliters of the glycerol gradient fraction containing the highest RdRp activity was treated with micrococcal nuclease, and in vitro transcription was performed in a 100-μl volume containing 40 mM Tris-HCl (pH 9.0); 8.0 mM $MgCl_2$; 2.5 mM dithiothreitol; 0.8 mM ATP, GTP, and CTP; 10 μCi of [α-^{32}P]UTP (ICN); 2% (vol/vol) ethanol; and 125 ng of actinomycin D as described previously (3), except that the incubation time was doubled from 30 min to 1 h. Five micrograms of the wild-type (wt) RNA and an equimolar amount of the other RNA fragments were used in both a standard RdRp assay and a competition experiment. The reaction products were analyzed by gel electrophoresis on an 8 M urea–polyacrylamide gel under denaturing conditions. [α-^{32}P]UTP incorporation was determined by Čerenkov counting of the reaction product in the gel. The transcription efficiencies of the various templates were calculated by dividing the counts per minute by the number of U residues present in the negative-sense reaction product, assuming that the 3′-terminal A residue was not being transcribed. Relative efficiency was obtained by comparing the calculated transcription efficiency with that of the unmodified reference template.

Construction and synthesis of the 83-nt fragment and 5′-to-3′ deletion mutants. The 5′-to-3′ deletion mutants (the 44-nt, G+30, 28-nt, and G+20 fragments) constructed were created by cloning of a corresponding oligonucleotide

* Corresponding author. Mailing address: Leiden Institute of Chemistry, Leiden University, P.O. Box 9502, 2300 RA Leiden, The Netherlands. Phone: (31)715274769. Fax: (31)715274340. E-mail: c.pley@chem.leidenuniv.nl.

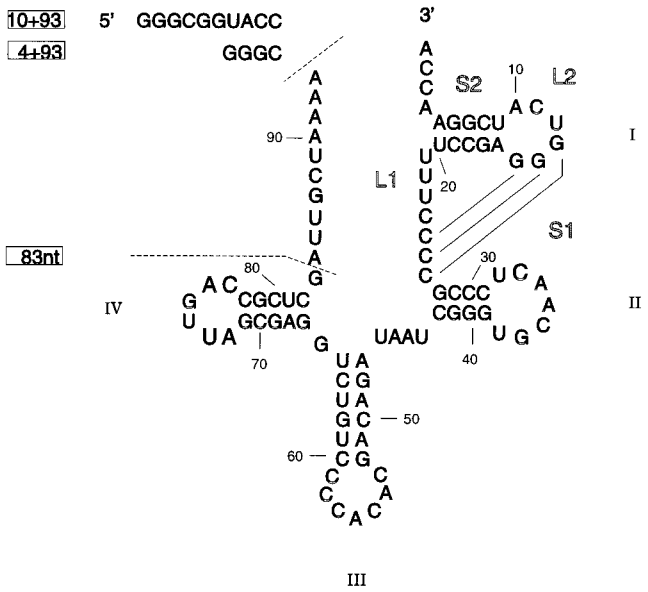

FIG. 1. Secondary structure of the 83-nt, 4+93, and 10+93 fragments containing the 3′ end of TYMV RNA. The 5′ end of the viral part of the different fragments is indicated by the broken lines. In the 4+93 and 10+93 fragments, the different nonviral sequences, 4 and 10 nt, respectively, are represented upstream of the broken line. Numbering of the nucleotides and hairpins is from the 3′ end. Numbering of the hairpins is indicated in roman numerals. The pseudoknot formation is indicated by solid lines. The stem regions, S1 and S2, and loop sequences, L1 and L2, of the pseudoknot are indicated.

behind a synthetic T7 promoter in the vector pUC19 as described elsewhere for the 83-nt fragment (3). The cDNAs were digested with *Mva*I, resulting in an RNA fragment with a 3′ CCA end after runoff transcription with T7 RNA polymerase. The RNA was purified by electrophoresis on an 8 M urea–15% polyacrylamide gel. The RNA concentration was determined by UV spectroscopy at 260 nm.

Construction and synthesis of the 4+93 and 10+93 fragments and pseudoknot mutants. The construction of the 4+93 and 10+93 fragments earlier designated wt(93+4) and wt(93+10), respectively, and the pseudoknot mutants was described previously (11, 12).

Isolation of 5S rRNA. The 23S and 5S rRNAs were isolated from the ribosome 50S subunit fraction of *Escherichia coli*. The RNAs were separated on a 2% agarose gel, and the 5S rRNA was isolated from the gel by diffusion at 4°C for 16 h.

Isolation of tRNA^{Phe} from yeast. Partially purified tRNA^{Phe} was obtained from a crude tRNA mixture from brewer's yeast as previously described (13).

Construction and synthesis of the 3′-terminal 208-nt fragment of AMV RNA 3. Plasmids pTE7 and pBRWT, both described previously (19), were used to construct plasmid ΔpΔHpACO, containing the 3′-terminal 208 nt of alfalfa mosaic virus (AMV) RNA 3 downstream of a synthetic T7 promoter and upstream of a *Pst*I site. Plasmid pTE7, containing the 3′-terminal 208 nt of AMV downstream of a pBR322 sequence of 783 nt and a T7 promoter sequence, was first digested with *Hin*dIII and *Pst*I to remove the nonviral pBR322 sequence. The remainder of the plasmid was then closed by blunt-end ligation. The plasmid obtained, ΔpΔHp, can be linearized by *Sma*I digestion, resulting in an RNA fragment with two nonviral 3′ C residues after transcription with T7 RNA polymerase. To remove the two nonviral C residues as a last step to obtain ΔpΔHpACO, ΔpΔHp was digested with *BstX*I and *Sma*I, and the *BstX*I-*Sma*I fragment was replaced by the corresponding fragment of pBRWT. Plasmid pBRWT contains the same sequence as pTE7, but the *Sma*I restriction site is changed in order to obtain a *Pst*I site just downstream of the viral sequence and upstream of the *Sma*I site. Linearizing ΔpΔHpACO with *Pst*I will now result in an RNA fragment containing the 3′-terminal 208 nt of AMV with the correct 3′ terminus after transcription with T7 RNA polymerase.

RESULTS

The 3′-terminal fragments containing the pseudoknot sequence possess sufficient information for efficient transcription. Deletion mutant forms of the 83-nt fragment were constructed in the 5′-to-3′ direction in order to investigate the importance of the tRNA-like structure in minus-strand initiation (Fig. 2B). All constructs, except for the G+20 fragment, contain the sequence which is folded into the 3′-terminal pseudoknot structure which is part of the aminoacyl acceptor arm of the tRNA-like structure (Fig. 1).

The glycerol gradient-purified and micrococcal nuclease-treated RdRp preparation was used to test these fragments as templates in in vitro RdRp assays. Figure 2A and Table 1 show that the 3′-terminal fragments containing the pseudoknot sequence, i.e., the 44-nt, G+30, and 28-nt fragments, all function more efficiently as templates than the 83-nt fragment. In the calculation of relative efficiency as described in Materials and Methods, it was assumed that the A residue present at the 3′ end of all transcripts was not being transcribed. This assumption is based upon the results obtained for brome mosaic virus (BMV) (14) and is supported by the results obtained for TYMV so far (1, 15, 17). Although for all of the tRNA-like fragments discussed in this paper, wrongly neglecting the 3′ A residue hardly has any influence on the percentages obtained, this is not completely true for the 5′-to-3′ deletion mutants. Therefore, the percentages obtained by including transcription of the terminal A residue in the calculations are also presented.

Surprisingly, the 3′-terminal hairpin (G+20 fragment) could also be used as a template by the RdRp (Fig. 2A and Table 1). However, a reduction of transcription efficiency to approximately 50% was observed. This twofold reduction indicates that the part of the pseudoknot upstream of the 3′ hairpin is important for efficient transcription but probably because of the resulting structure rather than base-specific interactions of the RdRp with these nucleotides; as in the latter case, a more drastic reduction was expected. This idea is strengthened by the low conservation of the nucleotide sequence in loop L1 of other TYMV tRNA-like structures (12).

Although the RdRp preparation was shown to be specific for TYMV RNA (3), this had to be tested again when using small RNA fragments. Table 1 shows that tRNA^{Phe} from yeast, 5S rRNA from *E. coli*, and the 3′-terminal 208 nt of AMV RNA 3, obtained by T7 RNA polymerase transcription of the cDNA clone, are all very poor templates for the RdRp in comparison with the 83-nt fragment. In the case of tRNA^{Phe}, some very small products, up to about 10 nt long, were detected after a long exposure (result not shown). It is very likely that modifications in this RNA prevent the synthesis of full-length minus strands. For AMV, it was previously shown that the complete genomic RNA could be used as a template, although at a low level compared with genomic TYMV RNA (3). The reason for this difference in behavior with the small 3′-terminal RNA fragment is not known.

The reaction products all migrated more slowly in an 8 M urea–15% polyacrylamide gel under denaturing conditions than the template RNA. This is in agreement with what was described previously for the reaction product of the 83-nt fragment (3). Treatment of this reaction product with nuclease S1 showed that the reaction product was double stranded (3). Therefore, we assume that the reaction products presented here also form very stable duplex RNAs with their templates, explaining the deviation in migration behavior in comparison with the template RNA.

The nucleotides of loop L2 (5′ UCA 3′), crossing the shallow groove of the quasicontinuous RNA double helix of the pseudoknot, are highly conserved in TYMV tRNA-like structures and are probably exposed to the solvent (12). As the nucleotides of this loop are still present in the G+20 fragment, although probably in a different conformation, mutational analysis of these bases could reveal base specificity of this loop

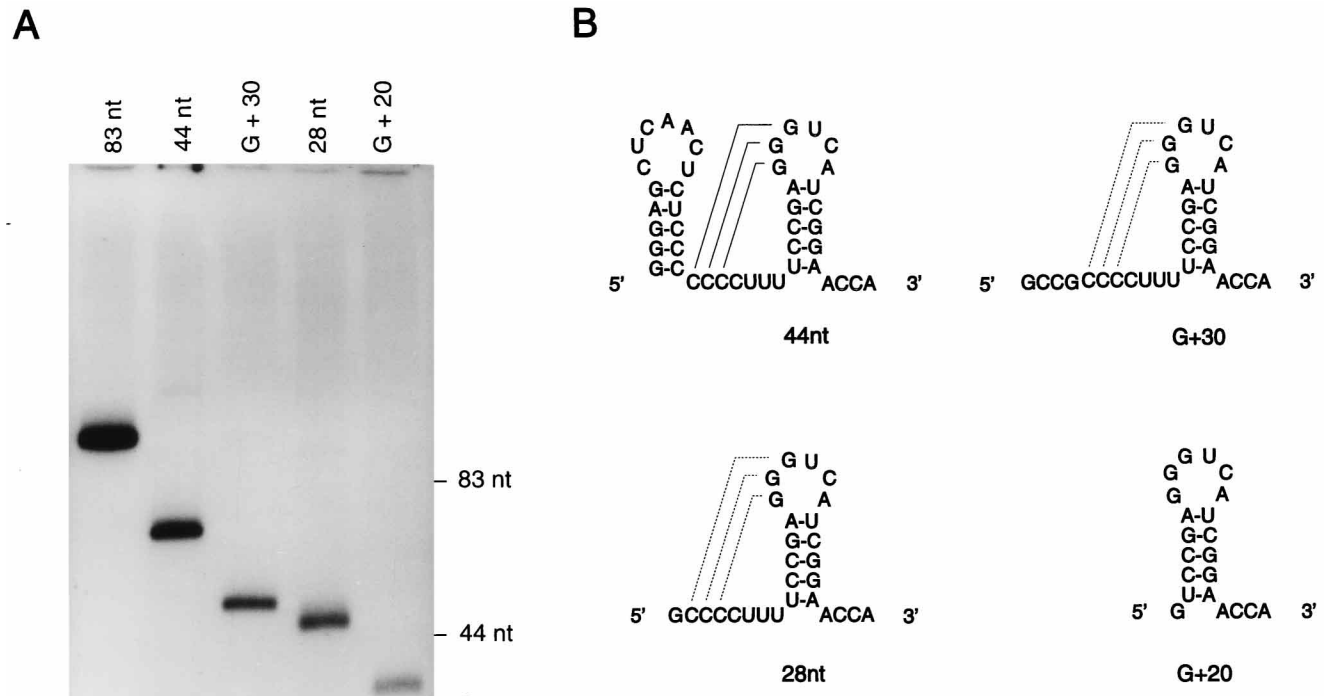

FIG. 2. Transcription of the 83-nt fragment and the 5′-3′ deletion mutants. (A) Autoradiography of the ^{32}P-labelled products using the 83-nt, 44-nt, G+30, 28-nt, and G+20 fragments as templates. The positions of the template RNAs, determined by staining, are indicated on the right. Numbers in the designations indicate the number of viral nucleotides from the 3′ end, and G+ means that a nonviral G residue is added at the 5′ end for transcription with T7 RNA polymerase. In the 44-nt fragment, the viral hairpin upstream of the pseudoknot has been replaced with a more stable nonviral hairpin. By nuclear magnetic resonance studies, it was shown that in the presence of 10 mM $MgCl_2$, the pseudoknot is indeed present in this fragment (23). (B) Secondary structures of the different template RNAs. The pseudoknot formation is indicated by solid lines. Broken lines indicate that the pseudoknot formation is putative.

in transcription. The A residue 10 nt upstream of the 3′ end (A10) and the U residue 12 nt from the 3′ end (U12) seem to be especially good candidates for base-specific interactions of the RdRp, as C11 is not always present in L2 loops of related viral RNAs (12).

Mutational analysis of the pseudoknot structure. Previously, the 3′-terminal 93 nt of TYMV RNA were cloned behind a T7 promoter and fragments 4+93 and 10+93, having 4 and 10 different nonviral nt at the 5′ end, respectively, were synthesized (Fig. 1). Site-specific mutations were introduced in the various parts of the pseudoknot in order to gain further insight into the stability of the RNA pseudoknot in the tRNA-like structure and the relationship to aminoacylation activity (11, 12). As both the 4+93 and 10+93 fragments turned out to be good templates for the RdRp in vitro compared with the 83-nt fragment (Table 2), we decided to use these mutants to further investigate the importance of the pseudoknotted structure in the initiation of minus-strand synthesis. We divided the mutants into three groups: (i) those with deletion mutations in loop L1 and L2 and an insertion mutation in L1, all derived from the 10+93-construct; (ii) those with substitution mutations in L2 and stem S1; and (iii) those with double mutations in S1, both derived from the 4+93 construct.

(i) Deletion and insertion mutations in L1 and L2. Figure 3 summarizes the L1 and L2 deletion mutants and the L1 insertion mutant used in this study. Table 2 shows that two- and three-nucleotide reductions of L1 (ΔU22U23 and ΔU21-U23, respectively) did not significantly influence transcription efficiency compared to that of the wt 10+93 fragment. This is in agreement with the low conservation of these nucleotides in the pseudoknot of the tRNA-like structures of related TYMV RNAs as mentioned above. However, deletion of all four nucleotides (ΔU21-C24) led to a decrease in transcription effi-

TABLE 1. Transcription efficiencies of the 83-nt fragment, the 5′-3′ deletion mutants, and RNA fragments of different origins[a]

Template	Relative efficiency (%)[b]
83-nt fragment	100 (100)
44-nt fragment	101 (94)
G+30 fragment	102 (87)
28-nt fragment	112 (95)
G+20 fragment	53 (45)
$tRNA^{Phe}$	<1
5S rRNA	<1
AMV 3′ RNA	<1 (<1)

[a] [^{32}P]UMP incorporation was determined by Čerenkov counting of the reaction products in the gel and was divided by the number of UMP residues present in the negative-sense reaction product, assuming that the 3′-terminal A was not being transcribed.

[b] Compared with the 83-nt fragment. Values are averages of two experiments. Errors in percentages are about 5%. For the values in parentheses, transcription of the terminal A residue was included in the calculations.

TABLE 2. Transcription efficiencies of pseudoknot mutants

Reference or test template	Relative efficiency (%)[a]		
	I	II	III
Wt 10+93[b]			100
ΔC11		77	
ΔC11U12		62	
ΔU22U23			106
ΔU21-U23			92
ΔU21-C24		62	
i4A		58	
83 nt			105
Wt 4+93[c]			100
A10→G			104
A10→C			99
U12→G	55		
U12→C			92
G14→C	53		
R1			90
R2			98
R3		60	
R4		66	
83 nt			120

[a] I, no pseudoknot expected; II, unstable pseudoknot expected; III, pseudoknot expected.

[b] The 10+93 fragment was the reference for the group of templates listed just below it. The values are averages of three experiments. Errors in percentages are about 5%.

[c] The 4+93 fragment was the reference for the templates listed below it. The values are averages of three experiments. Errors in percentages are about 5%.

ciency to about 60% (Table 2). Although earlier structure-probing experiments suggested that none of these deletions disrupts the RNA pseudoknot, a distortion of the structure of mutant ΔU21-C24 was certainly expected and was supported by the loss of aminoacylation of this mutant (12). The reduction of transcription efficiency could therefore be explained in the same way.

Insertion of four A residues between U21 and U22 (i4A) also resulted in a decrease of transcription efficiency to about 60% (Table 2). Structural analysis showed the existence of the RNA pseudoknot (12), and distortion of the pseudoknot structure is not expected for this mutant. However, studies on aminoacylation of this mutant do indicate that the enlarged L1 loop does sterically hinder the valyl-tRNA synthetase in binding of the tRNA-like structure. The same explanation may hold for the reduction of transcription efficiency of this mutant by the viral RNA polymerase.

Deletion of only C11 (ΔC11) resulted in a reduction of transcription efficiency to about 80% (Table 2). Deletion of both C11 and U12 (ΔC11U12) resulted in a reduction to about 60% (Table 2). This relatively low reduction does suggest that no base-specific interactions between the RdRp and these nucleotides exist, despite the conservation of especially U12 in related pseudoknots. Although probing of the mutants did not reveal disruption of stem S1 or S2, distortion of the pseudoknot structure may take place in the ΔC11 mutant and is certainly expected in the ΔC11U12 mutant (12). This, therefore, could explain the reduced transcription efficiency of both mutants. The complete loss of aminoacylation of both mutants is in agreement with this explanation.

(ii) Substitution mutations in L2 and S1. As C11 is not absolutely conserved in loop L2 of other TYMV RNAs, only residues A10 and U12 of L2 in the 4+93 fragment were replaced (Fig. 4B). Some of the substitutions do have an important effect on the structure, as concluded from structure probing (12) and as presented in Fig. 4B. Figure 4A and Table 2 show the reaction products and the transcription efficiencies, respectively, of these mutants compared to that of the wt 4+93 fragment. Replacement of A10 with a G or C residue or U12 with a C residue did not have much influence on transcription efficiency. In the A10→G and U12→C mutants, no considerable structural changes were detected by structure probing (12). In the A10→C mutant, an equilibrium between the pseudoknot structure and a structure in which S2 is stabilized at the top by an extra C-G base pair was proposed and in both conformations the stacking of the base pairs is comparable (12). As we used a large excess of RNA in our RdRp assays, it is not clear whether both conformations can be used as templates by the RdRp. Together, these results do indicate that both nucleotides do not interact with the RdRp in a specific way. Interestingly, all three mutants could not be aminoacylated (A10→C) or could be aminoacylated only at a low level (A10→G and U12→C) (12).

Replacement of U12 with a G residue resulted in a decrease in transcription efficiency of about 50% (Table 2). In this case, S1 is stabilized by an extra G-C base pair, as evidenced by structural probing (12). This shortening of L2 may, in turn, lead to a partial distortion of stem S2 in favor of one or two extra base pairs in S1. A similar result was obtained upon replacement of G14 with a C residue in order to investigate the influence of direct destabilization of stem S1, as proven by structural probing (12), on template activity. Again, these two mutants could not be aminoacylated (G14→C) or could be aminoacylated only at a very low level (U12→G) (12).

(iii) Double mutations in S1. The disrupted pseudoknot structure of the G14→C mutant could be restored by changing C26 into a G residue (12). Testing of this revertant (R1 in Fig. 5) in an in vitro RdRp assay resulted in a transcription efficiency almost as high as that obtained for the wt 4+93 fragment (Table 2). Three more double mutants in which S1 could be retained (R2, R3, and R4 in Fig. 5) were tested for transcription efficiency. Table 2 shows that changing the G14-C26 base pair into an A-U base pair did not have any influence on transcription efficiency. However, changing the G15-C25 base pair into an A-U base pair reduced the transcription efficiency in both R3 and R4 to about 60%. Structure probing of R4

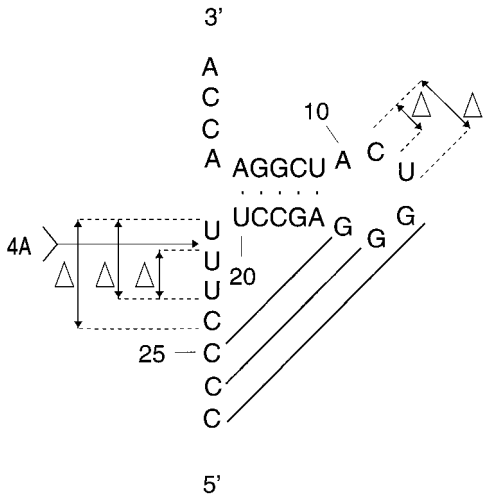

FIG. 3. Summary of the deletion mutations in L1 and L2 and the insertion mutation in L1 of the pseudoknot of the 10+93 fragment. The regions between two dotted lines connected by two-headed arrows were deleted, as indicated by the symbol Δ. The long, horizontal arrow indicates where four A residues were inserted.

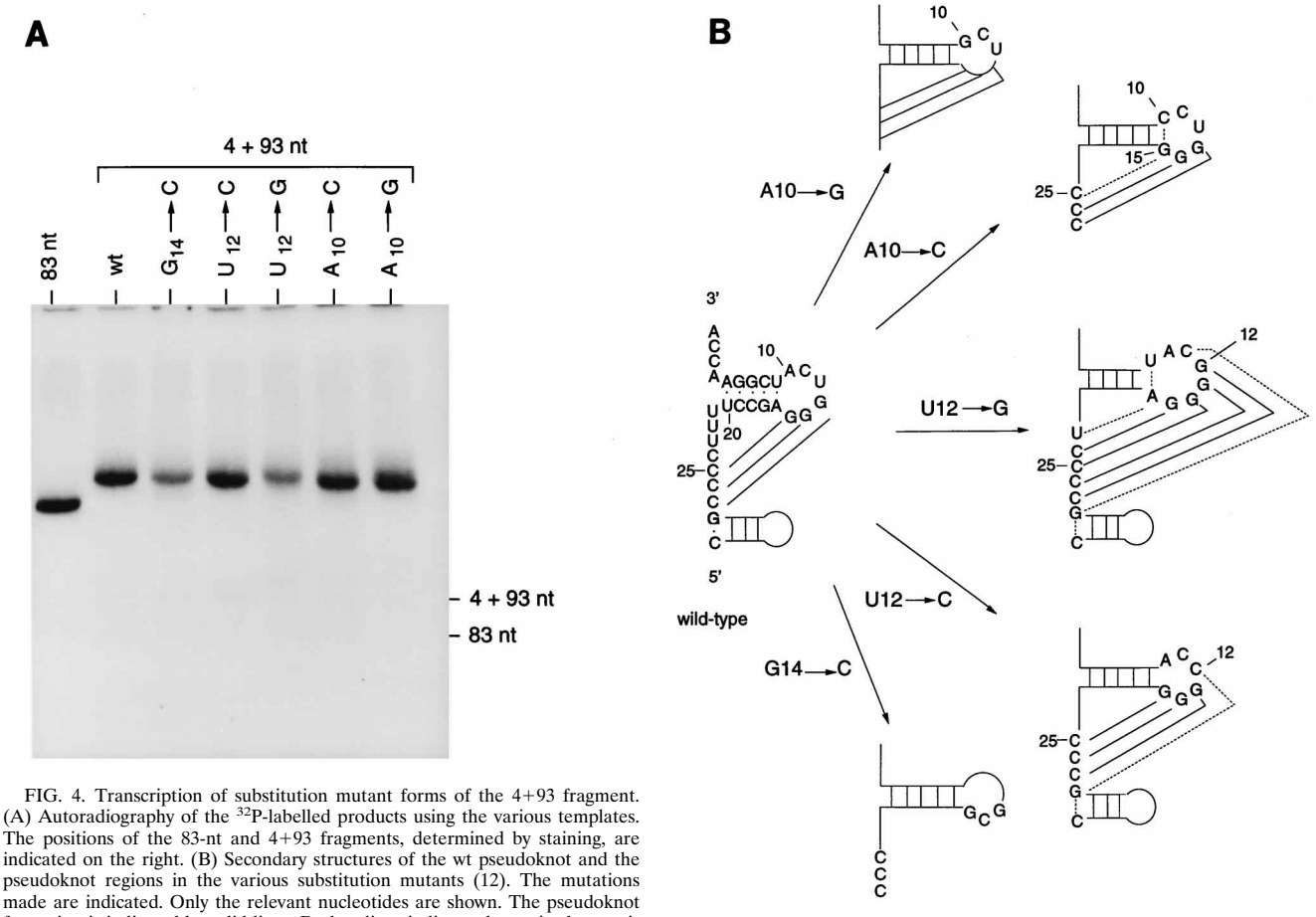

FIG. 4. Transcription of substitution mutant forms of the 4+93 fragment. (A) Autoradiography of the ^{32}P-labelled products using the various templates. The positions of the 83-nt and 4+93 fragments, determined by staining, are indicated on the right. (B) Secondary structures of the wt pseudoknot and the pseudoknot regions in the various substitution mutants (12). The mutations made are indicated. Only the relevant nucleotides are shown. The pseudoknot formation is indicated by solid lines. Broken lines indicate alternative base pair possibilities.

indicated the absence of a pseudoknot structure (12), while probing of R2 gave rise to contradictory results, in that an equilibrium between a pseudoknotted structure and a non-pseudoknotted structure was observed (12). As R3 is less stable than R2, a pseudoknot structure was not expected in this revertant. The fact that all of the double mutants could be aminoacylated, R1 to the wt level and R2, R3, and R4 to a lower level, was explained by assuming that the synthetase was able to stabilize the pseudoknot (12).

Competition between the 83-nt fragment and the substitution mutants. The most interesting results so far, compared to the results of aminoacylation, are those obtained by replacing nucleotides 10 to 12 of L2. We therefore decided to test these mutants again in a competition experiment with the 83-nt fragment in order to optimize the conditions to determine transcription efficiency. All of the mutants in the competition experiments reacted in a way similar to the way they did in the normal RdRp assays (compare Fig. 6 and 4A). However, when calculating the transcription efficiencies of the mutants in comparison with that of the wt 4+93 fragment, some minor differences were detected (Table 3, column A). The transcription efficiencies of both A10 mutants showed a reduction to about 80%, indicating that some minor structural changes, in comparison with the structure of the wt 4+93 fragment, prevail in these mutants. Such an effect was not detected in the U12→C mutant. For the U12→G and G14→C mutants, reduction of transcription efficiency was again observed. In the U12→G mutant, the relative efficiency even dropped to about 40% in comparison with that of the wt 4+93 fragment.

Surprisingly, when efficiency in comparison with the total amount of the reaction product was calculated, a significant

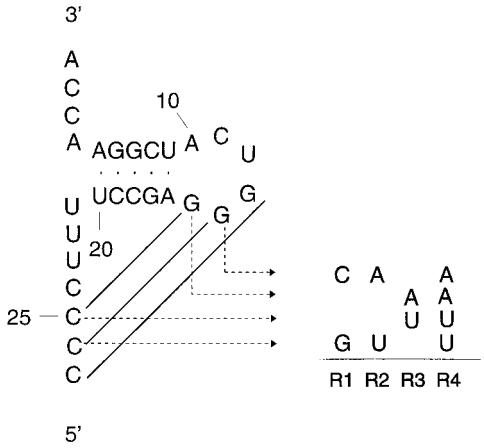

FIG. 5. Summary of the double mutations in S1 of the pseudoknot. The double mutations in revertants R1 to R4 are indicated on the right. The positions of the mutations are indicated by broken arrows. The pseudoknot formation is indicated by solid lines.

TABLE 3. Transcription efficiencies of substitution mutants in competition with the 83-nt fragment

Template	Relative efficiency (%)	
	A[a]	B[b]
Wt 4+93	100	34
A10→G	78	26
A10→C	78	26
U12→G	42	14
U12→C	94	31
G14→C	56	19

[a] Compared with total incorporation obtained from both the pseudoknot mutants and the 83-nt fragment and compared with the 4+93 fragment.
[b] Compared with total incorporation (100%). Relative efficiency of 83-nt fragment per assay = total incorporation − value in column B.

reduction was detected, even for the wt 4+93 fragment (Table 3, column B). This could indicate that the nucleotides of the 4+93 fragment upstream of the tRNA-like structure, although mostly of viral origin, do negatively influence the accessibility of the RdRp to the template.

DISCUSSION

This paper shows that the complete tRNA-like structure at the 3′ end of TYMV RNA is not needed for efficient transcription by the RdRp in vitro and therefore probably does not play a direct role in the replication of the viral RNA. On the other hand, the pseudoknot at the 3′ end of the tRNA-like structure is important, although not essential, as disruption of the pseudoknot structure results in a twofold reduction of transcription efficiency.

Various RNA fragments with mutations in the pseudoknot of the tRNA-like structure were tested for the ability to function as templates for the RdRp of TYMV. Previously, the same mutants were tested for valine acceptance and the effect of these mutations on the pseudoknot structure was determined by structure probing (12). Combining the new data with those previously obtained results in a better understanding of the function of the pseudoknot at the 3′ end of TYMV RNA, as will be discussed below.

Loop region L1 does not interact with the RdRp or valyl-tRNA synthetase in a specific way. Deletion of two or three nucleotides of L1 does not have much influence on transcription efficiency or on aminoacylation in vitro (12). Surprisingly, TYMV variants with only one C residue left in L1 could not multiply in protoplasts or could multiply only at a very low level (5). This indicates that the length of L1 is important, but probably in a process different from aminoacylation and transcription. Deletion of the four nucleotides of L1 appeared to reduce the transcription efficiency to about 60% (Table 2). As aminoacylation of this mutant is also lost (12), this can very well be explained by serious distortion of the pseudoknot structure. In conclusion, no base-specific interaction with RdRp or with valyl-tRNA synthetase is expected in this loop.

Loop region L2 has specific interactions with valyl-tRNA synthetase but not with the RdRp. Remarkably, the effect on transcription efficiency and aminoacylation observed for the mutations in L2 was different. Whereas deletion of residue C11 resulted in complete loss of aminoacylation (12), the transcription efficiency was only slightly reduced. This slight reduction could point to a small structural change, but whether it is sufficient to completely inhibit aminoacylation or whether base-specific interactions with the synthetase are involved is not known. Substitution mutations indicated that residues A10 and U12 do not interact with the RdRp in a base-specific way, although they appeared to be very important for the binding of the valyl-tRNA synthetase (12). However, some reduction of transcription efficiency is obtained when the A10 substitution mutants were tested in the presence of the 83-nt fragment in a competition experiment, indicating that a small structural change may also occur in these mutants. This could again be the reason for the drastically reduced aminoacylation of these mutants. Such an effect was not observed for the U12→C mutant in competition with the 83-nt fragment, indicating that this mutation does not alter the overall structure and that therefore the reduced aminoacylation activity must be due to specific interactions with the synthetase.

A stable pseudoknot structure is important for both aminoacylation and transcription. In both the U12→G and G14→C mutants, disruption of the pseudoknot structure was proven by structure-probing studies (12) and could very well explain the reduced transcription efficiency and aminoacylation. For transcription, the disruption in the U12→G mutant seems to be more drastic than that in the G14→C mutant, as in a competition experiment the efficiency of the U12→G mutant dropped even more, to about 40% (Table 3). In the G14→C mutant, S1 is disrupted but S2 still exists. In the U12→G mutant, S1 is stabilized and destabilization of S2 is expected. This may indicate that the stability of S2 is important for the interaction of the RdRp with its template.

The results obtained with revertants R1 to R4 show that the stability of S1 is important for efficient transcription, as it was for efficient aminoacylation. However, as these revertants can still be aminoacylated, although at a lower level, it was suggested that the synthetase is able to stabilize the pseudoknotted structure, especially in R3 and R4 (12). The RdRp does not

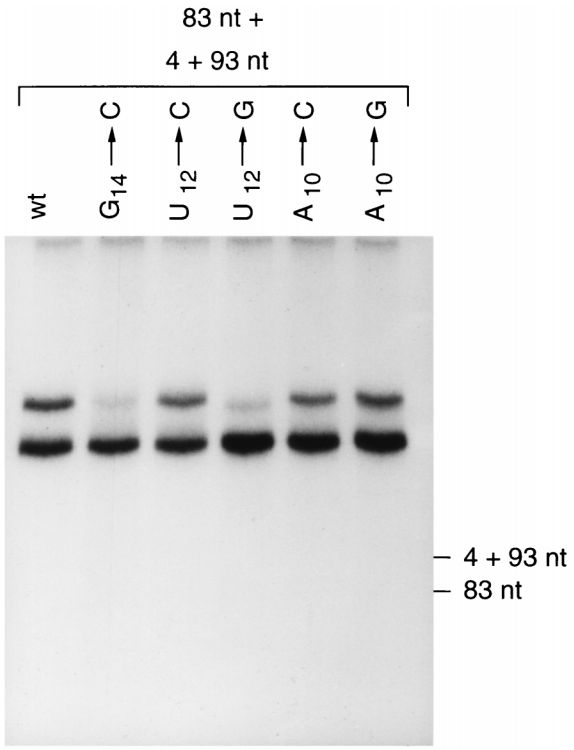

FIG. 6. Transcription of the substitution mutants in competition with the 83-nt fragment. Autoradiography of the ^{32}P-labelled products using the various templates. The positions of the 83-nt and 4+93 fragments, determined by staining, are indicated on the right.

seem to be able to achieve this, again indicating that the RdRp does not have any specific interactions with L1, L2, or S1 of the pseudoknot.

The importance of the pseudoknot in minus-strand synthesis is due to its structure. In conclusion, as the RdRp of TYMV does not have any base-specific interaction with L1, L2, or S1 of the pseudoknot, the importance of this part of the tRNA-like structure for efficient transcription must be due to its overall structure rather than its nucleotide sequence. On the other hand, the valyl-tRNA synthetase seems to have specific interactions, especially with L2 of the pseudoknot. Both the RdRp and the valyl-tRNA synthetase are sensitive to destabilization of the pseudoknot structure. However, absence of the pseudoknot structure, as in the G14→C mutant and most convincingly in the 3′-terminal hairpin (G+20 fragment), only results in a twofold reduction of transcription efficiency. The question that remains is which features of the 3′-terminal hairpin are responsible for the remaining promoter activity.

For BMV, it was previously shown that sequence alterations in most parts of the tRNA-like structure, especially in the putative anticodon-containing arm, decreased minus-strand synthesis (2, 4). However, destabilization of only the pseudoknot structure also resulted in low promoter activity (4). An important difference between both tRNA-like structures is that in BMV, besides the very 3′ end, part of the 5′-proximal region is also involved in the formation of the pseudoknot, whereas in TYMV the pseudoknot is formed by the very 3′ end only. Mutations outside the pseudoknot region of the tRNA-like structure of BMV RNA may alter this positioning of the 5′ and 3′ regions and thereby influence transcription efficiency.

Although the isolation and purification procedure we developed to obtain the RdRp of TYMV is relatively simple, it cannot be ensured that the replicase complex obtained is identical to that which functions in vivo. The possibility of loss of one or more protein subunits of viral or host origin, especially during solubilization from the chloroplast membrane, cannot be excluded. This could very well influence the specificity of the replicase. Besides this, the RdRp is obtained from the membrane-containing fraction of the cell, bound to its endogenous RNA, which is suggested to be of negative polarity (16). As it is unknown whether the same replicase complex is responsible for both minus- and plus-strand production, the protein composition of the RdRp we use to transcribe positive-sense RNA may differ from that of the RdRp responsible for this function in vivo.

Speculation and discussion are going on concerning the identity and function of host factors in the replication of plant viral RNAs containing a tRNA-like structure (7). Especially tRNA-specific proteins are expected to be involved. For TYMV, such a protein has not been found. The absence of such a protein in our RdRp preparation could explain why the complete tRNA-like structure is not necessary for efficient transcription in vitro.

ACKNOWLEDGMENTS

We thank Gied Jaspars for stimulating discussions and reading the manuscript and Chantal Reusken for the construction of plasmid ΔpΔHpACO. This work was performed under the auspices of the BIOMAC Research School of the Leiden and Delft Universities.

REFERENCES

1. **Boyer, J. C., G. Drugeon, K. Séron, M. D. Morch-Devignes, F. Agnès, and A. L. Haenni.** 1993. *In vitro* transcripts of turnip yellow mosaic virus encompassing a long 3′ extension or produced from full-length cDNA clone harbouring a 2 kb-long PCR-amplified segment are infectious. Res. Virol. **144:** 339–348.
2. **Bujarski, J. J., T. W. Dreher, and T. C. Hall.** 1985. Deletions in the 3′-terminal tRNA-like structure of brome mosaic virus RNA differentially affect aminoacylation and replication *in vitro*. Proc. Natl. Acad. Sci. USA **82:**5636–5640.
3. **Deiman, B. A. L. M., K. Séron, E. M. J. Jaspars, and C. W. A. Pleij.** 1997. Efficient transcription of the tRNA-like structure of turnip yellow mosaic virus by a template-dependent and specific viral RNA polymerase obtained by a new procedure. J. Virol. Methods **64:**181–195.
4. **Dreher, T. W., and T. C. Hall.** 1988. Mutational analysis of the sequence and structural requirements in brome mosaic virus RNA for minus strand promoter activity. J. Mol. Biol. **201:**31–40.
5. **Dreher, T. W., C. H. Tsai, and J. M. Skuzeski.** 1996. Aminoacylation identity switch of turnip yellow mosaic virus RNA from valine to methionine results in an infectious virus. Proc. Natl. Acad. Sci. USA **93:**12212–12216.
6. **Gargouri-Bouzid, R., C. David, and A. L. Haenni.** 1991. The 3′ promoter region involved in RNA synthesis directed by the turnip yellow mosaic virus genome *in vitro*. FEBS Lett. **294:**56–58.
7. **Giegé, R.** 1996. Interplay of tRNA-like structures from plant viral RNAs with partners of the translation and replication machineries. Proc. Natl. Acad. Sci. USA **93:**12078–12081.
8. **Joshi, R. L., J. M. Ravel, and A. L. Haenni.** 1986. Interaction of turnip yellow mosaic virus Val-RNA with eukaryotic elongation factor EF-1α. EMBO J. **5:**1143–1147.
9. **Litvak, S., L. Tarrago-Litvak, and F. Chapeville.** 1973. Turnip yellow mosaic virus RNA as a substrate of the transfer RNA nucleotidyltransferase. II. Incorporation of cytidine 5′-monophosphate and determination of a short nucleotide sequence at the 3′ end of the RNA. J. Virol. **11:**238–242.
10. **Litvak, S., A. Tarrago, L. Tarrago-Litvak, and J. E. Allende.** 1973. Host elongation factor *in vitro* interaction with TYMV and TMV genome depends on viral tRNA amino-acylation. Nature New Biol. **241:**88–93.
11. **Mans, R. M. W., P. W. G. Verlaan, C. W. A. Pleij, and L. Bosch.** 1990. Aminoacylation of 3′ terminal tRNA-like fragments of turnip yellow mosaic virus RNA: the influence of 5′ nonviral sequences. Biochim. Biophys. Acta **1050:**186–192.
12. **Mans, R. M. W., M. H. van Steeg, P. W. G. Verlaan, C. W. A. Pleij, and L. Bosch.** 1992. Mutational analysis of the pseudoknot in the tRNA-like structure of turnip yellow mosaic virus RNA: aminoacylation efficiency and pseudoknot stability. J. Mol. Biol. **223:**221–232.
13. **Mesters, J. R., E. L. H. Vorstenbosch, A. J. de Boer, and B. Kraal.** 1994. Complete purification of tRNA, charged or modified with hydrophobic groups, by reversed-phase high-performance liquid chromatography on a C4/C18 column system. J. Chromatogr. **679:**93–98.
14. **Miller, W. A., J. J. Bujarski, T. W. Dreher, and T. C. Hall.** 1986. Minus-strand initiation by brome mosaic virus replicase within the 3′ tRNA-like structure of native and modified RNA templates. J. Mol. Biol. **187:**537–546.
15. **Morch, M. D., R. L. Joshi, T. M. Denial, and A. L. Haenni.** 1987. A new 'sense' RNA approach to block viral replication *in vitro*. Nucleic Acids Res. **15:**4123–4130.
16. **Mouchès, C., C. Bové, and J. M. Bové.** 1974. Turnip yellow mosaic virus RNA replicase: partial purification of the enzyme from the solubilized enzyme-template complex. Virology **58:**409–423.
17. **Mouchès, C., C. Bové, C. Barreau, and J. M. Bové.** 1975. TYMV-RNA replicase. *In vitro* transcription and translation of viral genomes. Colloq. INSERM **47:**109–120.
18. **Pinck, M., P. Yot, F. Chapeville, and H. Duranton.** 1970. Enzymatic binding of valine to the 3′ end of TYMV-RNA. Nature (London) **226:**954–956.
19. **Reusken, C. B. E. M., L. Neeleman, and J. F. Bol.** 1994. The 3′-untranslated region of alfalfa mosaic virus RNA 3 contains at least two independent binding sites for viral coat protein. Nucleic Acids Res. **22:**1346–1353.
20. **Rietveld, K., R. van Poelgeest, C. W. A. Pleij, J. H. van Boom, and L. Bosch.** 1982. The tRNA-like structure at the 3′ terminus of turnip yellow mosaic virus RNA. Differences and similarities with canonical tRNA. Nucleic Acids Res. **10:**1929–1946.
21. **Skuzeski, J. M., C. S. Bozarth, and T. W. Dreher.** 1996. The turnip yellow mosaic virus tRNA-like structure cannot be replaced by generic tRNA-like elements or by heterologous 3′ untranslated regions known to enhance mRNA expression and stability. J. Virol. **70:**2107–2115.
22. **Tsai, C. H., and T. W. Dreher.** 1991. Turnip yellow mosaic virus RNAs with anticodon loop substitutions that result in decreased valylation fail to replicate efficiently. J. Virol. **65:**3060–3067.
23. **van Belkum, A., P. J. Wiersema, J. Joordens, C. W. A. Pleij, C. W. Hilbers, and L. Bosch.** 1989. Biochemical and biophysical analysis of pseudoknot-containing RNA fragments: melting studies and NMR spectroscopy. Eur. J. Biochem. **183:**591–601.